

# Safety Control for Impedance Haptic Interfaces

Xue-Jian He\*, Kup-Sze Choi

Centre for Smart Health, School of Nursing  
The Hong Kong Polytechnic University, Hong Kong

\*Tel: 852-27664156; Email: [xjimhe@polyu.edu.hk](mailto:xjimhe@polyu.edu.hk); Fax: (852)2364-9663

**Abstract**— Instability in haptics-enabled systems due to behaviors of human operators or unknown virtual environments can present safety issues. If manipulated inappropriately, then a haptic stylus may be ejected with a velocity as high as 1.4 m/s as observed in our experiments. To prevent the harms that are caused by ejection, three safety control models are thus proposed. The first one is a simple controller based upon velocities and forces; and the others are derived from a grasp force model which exploits the state of the haptic stylus including accelerations, velocities and penetration forces to model the grasp force. Based on the force model, safety indicators called “safety observers” are proposed to closely monitor system instability caused by for instance sudden release of a haptic stylus from a user when interacting with virtual objects. In such a case, traditional control methods fail to trigger a protection mechanism. In contrast, the proposed safety controllers can generate appropriate damping forces to counteract system instability which is indicated by the “safety observers”. Experimental results show that the proposed models can effectively reduce the ejection velocities of a haptic stylus and stabilize the haptics-enabled system even in presence of active forces. Since prior knowledge of virtual environments and additional hardware sensors are not required, the proposed approaches have the potential to be widely adopted in haptics-enabled applications.

**Index Terms**— Safety control, Haptic rendering, Grasp force, Stability, Passivity, Impedance

## 1 INTRODUCTION

Most haptic systems are modeled with a two-port framework [1] where a haptic interface with two ports is connected between a human operator and a virtual environment to form a virtual coupling network. Unlike conventional robotic manipulators, haptic devices interact closely with human operators. As the devices actively generate physical energy, instabilities can damage hardware and even pose real dangers

to human operators [1-4]. Safety issues are of particular concerns to disabled users who often have slower defensive reflexes, relatively poor hand-eye coordination and diminished sensorimotor abilities that lead to higher risks in operating haptic devices as compared with able-bodied users [5]. Take the “virtual wall” experiment as an example as shown in Fig. 1. Suppose an indentation is to be made against the wall along the negative  $Z$  axis. Based on passivity analysis, the system is passive if and only if the energy flowing in exceeds the energy flowing out for all time. The energy difference is quantified with a metric, called “Passivity Observer” (PO) [6]. Here, when the stylus of the haptic device is indented against the wall, the wall is said to act passively while a positive PO value is observed. On the other hand, when the stylus is released suddenly, it will be ejected abruptly toward the user along the positive  $Z$  axis, where the system presents active behavior and a negative PO value is observed. The ejection velocities are in the range from 0.2 m/s to as high as 1.4 m/s within 0.02 s, as evidenced by experiments. This could be a potential danger to the user. Sudden release of haptic stylus during interactive virtual operations is not rare since users are often required to perform repetitive actions for extended period of time, e.g. rehabilitation practice, which is likely to lead to fatigue and results in unstable grasp of the haptic device. Other possible reasons of inadvertent release of haptic stylus include unfamiliarity with the manipulation of haptic devices and the virtual environment, as well as interruption or distraction during the operations.

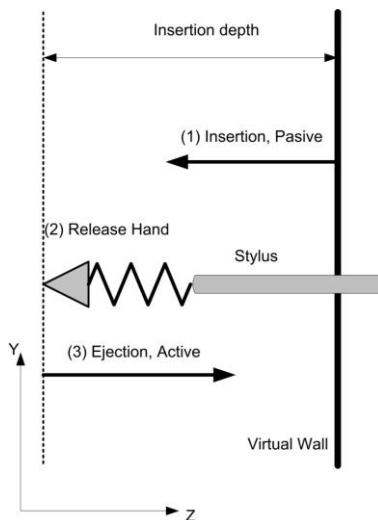


Fig. 1. Schematic diagram of the virtual wall experiment.

In previous studies, many researchers focused on haptic-stability analysis in haptic interface design [2, 6-10] to avoid potential threats to users. The instability of a haptic-enabled system is usually caused by undesirable energy imbalance or “energy leakage” [11], leading to oscillations and vibrations of the sys-

tem [12]. The stability of a haptic system depends on the human operator, virtual environment and haptic device, while the behavior of later two – human operator and virtual environment – are highly unpredictable [2]. For example, the operator’s maneuver in the virtual environment may destabilize the haptic system by reflecting excessive energy back into the system. A virtual environment may also exhibit active behavior even it is designed to be a passive system due to time delays caused by numerical integration schemes or network communication latency [13], or error resulting from quantization of human-device interactions [7, 14]. Hence, virtual environments are often “non-linear” and difficult to model.

Although non-linear control theory and parameter-based methods [3] have been employed for stability analysis of haptic devices, it is still challenging to completely avoid instability, in that they rely on the modeling of the behavior of the users, their hands or arms, which is difficult to be modeled. To tackle this issue, passivity analysis has emerged as an effective means for investigating the stability of both linear and non-linear systems [15]. Whereas, the passivity requirement is a more stringent condition than stability [12], i.e. a passive system is clearly stable or safe while a stable or safe system is not necessarily passive. For example, oscillations or vibrations may be required by or intentionally introduced into some haptically stable applications so that the haptic device can generate periodic and bounded oscillations around an operating point in a stable manner, i.e., a non-passive behavior [12]. In these active haptic systems, passivity control methods cannot be directly applied for safety control. Therefore, new safety-control algorithms that can be used in various haptics-enabled applications are yet to be developed.

In this paper, three safety indicators, namely the Velocity and Force Observer (VFO), Hand Grasp Observer (HGO) and the Windowing Safety Observer (WSO), are proposed to quantify the safety level of haptic systems. Based on these indicators, safety control strategies are developed and evaluated with experiments. Since the safety control strategies require no prior knowledge of the virtual environments, they are applicable to a wide range of applications. The rest of the paper is organized as follows. Previous work related to robotic and haptic safety is introduced in Section 2. In Section 3, the hand grasp force model, the proposed safety observers and the corresponding control strategies are presented. In Section 4, the experiments conducted to evaluate the effectiveness of the safety control strategies are explained. Lastly, discussions and conclusions are given in Section 5 and 6 respectively.

## 2 RELATED WORK

In this section, the related work on safety issues of interactions between machine and human is reviewed. Since the haptic interface as mentioned in the previous section is closely related to robots, the work on robotic safety is firstly reviewed. Then, the research related with haptic safety is introduced, mainly focused on virtual coupling and passivity analysis.

### 2.1 Robotic Safety

Though the interactions between human and industrial robots are well studied, the threats caused by the robots have not yet been fully eliminated, especially with the emergence of new robot applications [16]. In these new applications, humans and robots cooperate with each other to fulfill tasks in the same workspace. Industrial robots typically work alone in restricted areas to prevent any interactions harmful to humans; while in physical human-robot interactions (pHRI), the robots make constant contacts with humans. Traditional robotic controllers such as proportional-integral-derivative (PID) controllers may not be very suitable to the safety control [17]. The reported studies on solving safety issues in pHRI can be divided into two main approaches, namely, passive safety and active safety [18]. The approaches of passive safety resort to safe mechanical design, by reducing the manipulator link inertia and weight using lightweight but stiff compliant components to achieve intrinsic safety. On the other hand, research on active safety attempts to prevent collisions or reduce the effect of collision on users by using some controllers, e.g. impedance control [19] and optimal control schemes [20], or additional sensors, e.g. camera and a force/torque sensor [21].

The level of safety is usually measured quantitatively with some safety indices. Many of the indices have been proposed based on injury severity to develop safety controllers for industrial robots, e.g. the Gadd Severity Index (GSI) [22] and the Head Injury Criterion (HIC) [23]. These injury indices originate from the fields of automotive crash testing rather than robotics. Haddadin showed that classical severity indices established in the automobile industry cannot be transferred without modification to the field of robotics [24]. When applying these indices to pHRI applications, it is necessary to ensure the conditions under which these indices were developed are also satisfied for the robotics applications concerned [25].

Although safety regulations of industrial robots are well defined by standards such as ISO 10218 [26, 27], they are not readily extensible to pHRI applications (e.g. haptics-enabled systems), since the set-

tings, functions and working mechanisms of pHRI robots are different from that of industrial robots. In addition, the threats caused by robots are usually different from one system to another. Therefore, it remains a challenging task to design a generic safety algorithm that is applied to ensuring the safety of pHRI [16].

## 2.2 Haptic Safety

Very few studies focusing on haptic safety are reported in the literature. This could be explained by the fact that the haptic interfaces are usually relatively small and less powerful when compared with industrial robots, thus attracting fewer attentions from researchers. However, as mentioned in previous section, as haptic devices closely interact with users and high ejection velocity could be generated due to inappropriate operations or defective force-rendering algorithms. Therefore, reliable protection mechanisms are also needed here, in view of the notable trend that the technology is now pervading into various application domains. In previous work, researchers are dedicated to the design of algorithms that ensure forces are rendered stably and systems respond passively.

Virtual coupling is a widely used method for guaranteeing stability in haptics-enabled systems. It usually employs a combination of series and parallel elements interposed between the haptic device and the virtual environment to limit the impedance range presented by the virtual environment. The technique of virtual coupling between the haptic device and the virtual environment was first proposed by Colgate et al. [14]. The aim was to ensure the stability of a haptic simulation and decouple the haptic rendering loop running at a refresh rate of 1k Hz from the 30-Hz simulation loop. To achieve the desired decoupling effect, the haptic device must be unconditionally stable, and the human operator and virtual environment are supposed to be passive. While it is reasonable to assume that the operator is passive for stability analysis [28], the assumption of passive virtual environment is questionably since it is difficult to implement numerical integration routines that can strictly adhere to the physical laws that govern the simulation dynamics [2]. Another drawback of the virtual coupling is performance degradation due to excessive energy dissipation in some conditions [4]. It has been demonstrated that even if the virtual coupling is achieved for individual virtual environments to render a passive system, switching between different virtual environments can still lead to system instability [29]. An alternative virtual coupling method has also been developed based on the characterization of the energy exchange among the human operator, hap-

tic interface and the virtual environment [1]. This method can be applied to all causality combinations (admittance or impedance) and is less conservative than the passivity-based design. Optimal virtual coupling parameters are derived by using a dynamic model of the haptic device and satisfying Llewellyn's absolute stability criterion [30]. Though stable force rendering can be achieved by virtual coupling, safety remains an issue, which must be solved particularly when haptic interfaces are applied to applications like rehabilitation of motor skills.

Hannaford and Ryu introduced a passivity-control strategy based on a *passivity observer* and a *passivity controller* [6]. This approach relied on the energy variables directly and made use of an adjustable damping element to keep the system passive. The damping element was activated only when negative energy was observed and dissipation was necessary to achieve minimal damping. However, the time domain passivity controller suffers from sudden and often large force changes when the passivity condition is breached. To solve the problem, an energy-based time domain passivity control scheme was proposed [8], where *reference energy* was incorporated into the passivity observer to smoothen the controller output. Recently, a power-based time domain passivity controller was also proposed [10], where a stability condition based on power rather than energy was monitored, so that the passivity controller was activated more uniformly than that of the energy-based method. The issue caused by the sudden activation of the passivity controller was thus alleviated. Moreover, the power-based method did not require numerical integration in energy calculation and thereby avoiding error in the calculation. However, the time domain passivity controllers presented in [8, 10] are based on the assumption that the information of the models or virtual environments is known, which may not be the case with the wide variety of haptic applications, e.g., haptic playback system [31] and haptics-enabled tele-operation system [4]. Another issue of the passivity controllers is that it cannot be directly applied to those haptics-enabled systems with dynamic objects or active forces. Hence, in view of potential safety issues, robust algorithms are still needed for stable haptic rendering in unknown virtual environments.

### 3 METHODS

In this section, we first introduce a simple safety controller which is directly based on the velocities and forces of the haptic interface. However, the ejection velocity cannot be greatly reduced by the controller, as demonstrated in Section 4.4.1. Hence, two other controllers based the hand-grasp-force model are

proposed. Based on this model, two safety observers are developed, namely, hand grasp observer and windowing safety observer, followed by the corresponding control strategies.

### 3.1 Velocity and Force based Controller (VFC)

In traditional robotic safety control, the velocity of robots is closely monitored. If the velocity is very high and is beyond a certain threshold value, the corresponding protection mechanism will be invoked. However, the stylus of the haptic interface could be manipulated to move freely in the workspace at a speed as high as 1 m/s, as observed in experiments. If the safety controller cannot differentiate whether the high velocity is generated or not by the device, it can potentially create false alarms that misinterpret normal operations as risky high-speed actions, triggering unnecessary protection mechanism and disturbing the user. Hence, additional status of the haptic device, i.e. forces, is thus adopted here to distinguish normal operations from accident stylus ejection. The Velocity and Force based Observer (VFO) proposed for safety control is defined as,

$$S_{vf} = V \cdot F / (V_t \cdot F_t), \quad (1)$$

where  $V$  is the velocity of the stylus,  $F$  is the force calculated based on virtual wall model,  $V_t$  and  $F_t$  are the threshold values. The basic idea of the observer is that if the observed velocity and force are larger than the thresholds at the same time, the system is considered to be under an unsafe condition. Based on the observer, the safety controller is given by,

$$F_{vfc} = \begin{cases} -F_v - \mu \cdot V, & \text{if } S_{vf} > 1 \\ 0, & \text{else} \end{cases}, \quad (2)$$

where  $F_{vfc}$  is the control force,  $F_v$  is the penetration force generated by virtual-wall force model, and  $\mu$  is a damping constant. The first term ( $-F_v$ ) is to cancel the penetration force, while the second term ( $-\mu \cdot V$ ) is a damping force to reduce the ejection velocities and impacts.

### 3.2 Hand Grasp Force Model

The human hand is so dexterous that tiny changes in hand gestures or configurations can result in different dynamic behaviors [32]. An accurate model of the human hand is necessary not only to develop a stable haptic device, but also to implement a safe haptics-enabled application. The model is also critical for proper stability analysis, interface design, and improving haptic fidelity. Hence, a hand grasp force model – a dynamic model of the human hand – is proposed for the development of a safety control strategy for haptic systems. In the model, the haptic interface is regarded as a point mass and its dynamics is

governed by the following differential equation [9]:

$$mA + bV + c \cdot \text{sign}(V) = F_v + F_h, \quad (3)$$

where  $m$  is the physical inertia of the haptic interface,  $b$  is the viscous friction coefficient,  $c$  is the coefficient of dynamic Coulomb friction,  $A$  is its acceleration,  $V$  is its velocity,  $F_v$  is the force exerted to the haptic device by the virtual environment, and  $F_h$  is the force applied by a human operator. Therefore, the grasp force,  $F_h$  can be given by

$$F_h = mA + bV + c \cdot \text{sign}(V) - F_v. \quad (4)$$

### 3.3 Hand Grasp Observer

In order to monitor the hand grasp status, an indicator called Hand Grasp Observer (HGO),  $S_h$  is devised and defined by

$$S_h = \frac{|F_v|}{|F_h| + \alpha}, \quad (5)$$

where  $\alpha$  is a small positive force used to prevent division-by-zero error when  $|F_h|$  is zero (set to 0.001 N in the experiments), and  $|\cdot|$  is the absolute value operator. This indicator describes the hand grasp status using the relationship between the grasp force and the virtual environment. If the user grips the haptic stylus tightly when indenting against the virtual wall with a large depth  $D$ , the following approximation holds,

$$|F_h| \approx |F_v| = KD, \quad (6)$$

where  $K$  is the spring constant. Consequently,  $S_h$  approaches 1, meaning that the haptic stylus is grasped firmly and the system is under normal operations. If the hand releases the stylus suddenly, Eq. (6) does not hold anymore, where  $F_h$  equals zero and  $F_v$  is still calculated by the spring model with a penetration depth  $D$ . Then,  $S_h$  is approximated by

$$S_h \approx \frac{|F_v|}{\alpha}. \quad (7)$$

Since  $\alpha$  is small and  $|F_v| \gg \alpha$ ,  $S_h \gg 1$ . Hence, HGO can be used to monitor the hand grasp status for the purpose of safety control. We define that the status of the system is safe if the following criterion is satisfied,

$$S_h \leq \zeta, \quad (8)$$

where  $\zeta$  is a threshold ( $>1$ ) and the value is determined experimentally as 1.5. Note that if the threshold

value is close to 1, the controller will become too sensitive and disturb normal operations.

### 3.4 Windowing Safety Observer

Passivity analysis is also exploited in the proposed method to monitor hand grasp status. As discussed in Section 1, the passivity theory is widely used for stability control in haptics-enabled systems since it allows decoupling of the analysis of the mechanical haptic system from the properties of human operator. Based on the passivity analysis, the Safety Observer (SO)  $E_{so}$  is defined by (see Appendix for details),

$$E_{so}(n) = \Delta E(n) \approx \Delta T \sum_{i=1}^n F_h(i)V(i) - \frac{mV(n)^2}{2\eta}, \quad (9)$$

where  $m$  is the physical inertia of the stylus,  $\Delta T$  is a time step,  $V$  is the velocity of the haptic stylus,  $F_h$  is the estimated hand grasp force, and  $\eta$  is the energy ratio. Assuming initial energy storage is zero, the system is safe if and only if,

$$E_{so}(n) \geq \delta \Rightarrow \Delta T \sum_{i=1}^n F_h(i)V(i) - mV(n)^2/2\eta \geq \delta, \forall n \geq 1, \quad (10)$$

where  $\delta$  is an energy threshold of a negative value. A negative threshold value is adopted here as the safety requirement is a relaxed condition of passivity. When the accumulated energy entering into the system just decreases from a positive value to a negative one, the system begins to act actively. However, at that moment the system could still be safe because the user's grip could cancel out the active movement of the haptic stylus. Another reason for the negative threshold is that the safety condition can also be used in the system with active forces, which will be demonstrated in Section 4.5. The above equation states that the energy supplied to a safe system must be greater than a negative threshold for all time, which is similar to the principles in passivity analysis [1]. If the value of  $E_{SO}$  becomes a large negative value, the system will transit into an unsafe status. However,  $E_{SO}$  is insensitive to status changes of system safety. For example, consider a virtual environment which is very dissipative in location A and active in location B. If the user spends a lot of time interacting at A, then, SO may build up a large positive value of energy. Then, when the user moves over and interacts at location B, the Safety Controller (SC) based on SO will not be activated immediately until a certain amount of negative energy is produced and accumulated in the active region. In order to resolve the issue of energy accumulation and dissipation, a time-varying reference energy might be introduced in a way similar to that in passivity control strategy [8], which is defined based on the information of the model or virtual environment. Unfortunately, the

information might be not available in some cases. Inspired by the time-domain passivity controller in [6], a safety control strategy based on Windowing Safety Observer (WSO) is thus proposed in the paper, aiming to address the energy accumulation issue of unknown virtual environments. Similar to Eq. (10), the energy measured with WSO,  $E_{wso}$ , is defined by the following equation,

$$E_{wso}(n) = \begin{cases} \Delta T \sum_{i=n-w+1}^n F_h(i)V(i) - \frac{mV(n)^2}{2\eta}, & n \geq w \\ \Delta T \sum_{i=1}^n F_h(i)V(i) - \frac{mV(n)^2}{2\eta}, & n < w \end{cases}, \quad (11)$$

where  $w$  is the size (width) of a window. The energy within a specified time interval ( $w \cdot \Delta T$ ) is observed.

### 3.5 Safety Controllers

In [6], in order to maintain system passivity, a time-varying damper called Passivity Controller (PC) is used to dissipate only the required amount of energy so that overall passivity is maintained. The control force  $F_{pc}$  calculated by PC is defined by

$$F_{pc} = \begin{cases} -E_{so}/(V \cdot \Delta T), & \text{if } E_{so} < 0 \\ 0, & \text{if } E_{so} \geq 0 \end{cases}. \quad (12)$$

For simplicity, the temporal index  $n$  is removed in the above and following equations. However, this PC cannot be utilized for safety control since it cannot be applied to the systems involving active forces. To solve this issue, a safety control strategy based on WSO called Windowing Safety Controller (WSC) is proposed, as shown in Fig. 2. The control force of WSC,  $F_{wsc}$ , is defined by

$$F_{wsc} = \begin{cases} -F_v - \mu \cdot V, & \text{if } E_{wso} < \delta \\ 0, & \text{else} \end{cases}, \quad (13)$$

where  $\mu$  is a damping constant. The first term ( $-F_v$ ) is to cancel the penetration force, and the second term ( $-\mu \cdot V$ ) is proportional to the velocity of the haptic stylus, instead of inversely proportional to the velocity as in Eq. (12). This control strategy can avoid the instability that may occur when the observed energy fluctuates around zero and the stylus velocity is very small. From Eq. (12), it can be seen that if  $E_{so}$  has a negative value and the velocity  $V$  tends to zero, the control force will be very large and result in system instability. The WSC as defined by Eq. (13) has the spatially local feature of passivity monitoring that does not accumulate the large energy from previous stable regions. Consequently, it has better sensitivity of passivity control as compared with that of PC. At the same time, by introducing a negative energy threshold  $\delta$ , it makes the controller be applicable to those systems with active forces.

Similar to Eq. (13), a safety controller called Hand Safety Controller (HSC) based on HGO (Eq. (8)) is defined as,

$$F_{hsc} = \begin{cases} -F_v - \mu \cdot V, & \text{if } S_h > \zeta \text{ and } |F_v| > F_t, \\ 0, & \text{else} \end{cases}, \quad (14)$$

where  $S_h$  is defined by Eq. (5) and (8),  $F_t$  is a force threshold. The forces are combined with the HGO to determine the safety conditions. When the penetration force and grasp force are too small (e.g.  $< 0.1$  N),  $S_h$  may fluctuate considerably and create false alarms that trigger the protection mechanism needlessly. Considering that the ejection velocities are not large enough to become harmful when the penetration forces are small, force checking is also introduced in the controller.

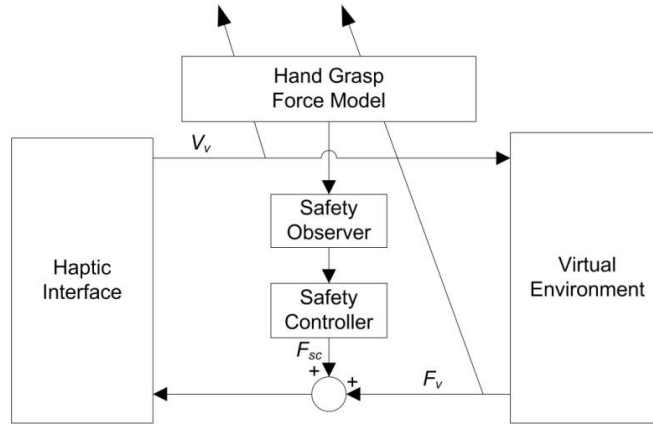


Fig. 2. Safety control based on the proposed hand grasp force model. The safety observer can be WSO or HGO, and the safety controller can be WSC or HSC.

## 4 EXPERIMENTS AND RESULTS

A number of experiments have been conducted to evaluate the effectiveness of the approaches proposed for haptic safety control. The stylus ejection experiment is first carried out to determine the model parameters and to study the maximum ejection velocities of a haptic stylus. Then, the performance of safety observers and control strategies are investigated. The proposed haptic safety control approaches are also evaluated for the haptic systems with active forces.

### 4.1 Stylus Ejection Experiments

The results of “virtual wall” experiment are commonly used as a performance benchmark for haptic systems since most interactions with virtual environments can be reduced to interactions with virtual wall of different stiffness and damping [1]. In the experiment, the tip (i.e., haptic interface point) of the haptic device stylus is pushed along the negative  $Z$  axis. If the stylus position in  $Z$  axis is less than zero, then the force  $F$  is calculated by,

$$F = K|z| - BV, \quad (15)$$

where  $K$  is the stiffness constant,  $B$  is the damping constant, and  $V$  is the stylus velocity. After the stylus reaches a depth  $D$ , it is withdrawn along the positive  $Z$  axis, as shown in Fig. 1. The system acts passively when the haptic stylus is pushed against the wall, while it acts actively when the stylus is withdrawn along the opposite direction. An experiment is designed with the virtual wall to test the safety monitoring and control strategies. As illustrated by Fig. 1, the experiment contains three steps. First, the haptic stylus is manipulated to push the tip penetrates into the virtual wall. After the tip reaches a depth  $D$ , the user then suddenly releases the stylus. Finally, the stylus is ejected backwards with a velocity due to the conversion of the potential energy stored in the first step into kinetic energy.

In this experiment, the haptic device, PHANTOM<sup>®</sup> Desktop<sup>™</sup> from the Sensable Technologies, is used (see Fig. 3). The device has 6 degree-of-freedom positional inputs and 3 degree-of-freedom force outputs. The inertia of the stylus (Eq. (3))  $m=0.157$  kg (estimated by the maximum ejection velocity of haptic stylus, to be discussed in Section 4.2),  $b=-0.005$  N·s/m and  $c=0.038$  N [9]. Fig. 4(a) plots the ejection velocity over time with  $K=200$  N/s and  $D=0.039$  m. Note that the value of stiffness is set so that the maximum ranges of forces and workspace of the used haptic device are not exceeded. It can be seen that the ejection velocity of the haptic stylus increases rapidly from 0.2 m/s to 1.2 m/s within about 0.02 s after it is released suddenly. The variations of insertion depth over time as shown in Fig. 4(b) indicate that the haptic stylus is ejected from  $Z=-0.039$  m to 0.1 m within 0.25 s after it is released. This experiment clearly demonstrates that the ejection can proceed at a high velocity that may pose great threats to the users. In what follows, further experiments will be presented regarding the estimation of model parameters that associate with the maximum ejection velocity.



Fig. 3. The PHANTOM<sup>®</sup> Desktop<sup>™</sup> haptic device.

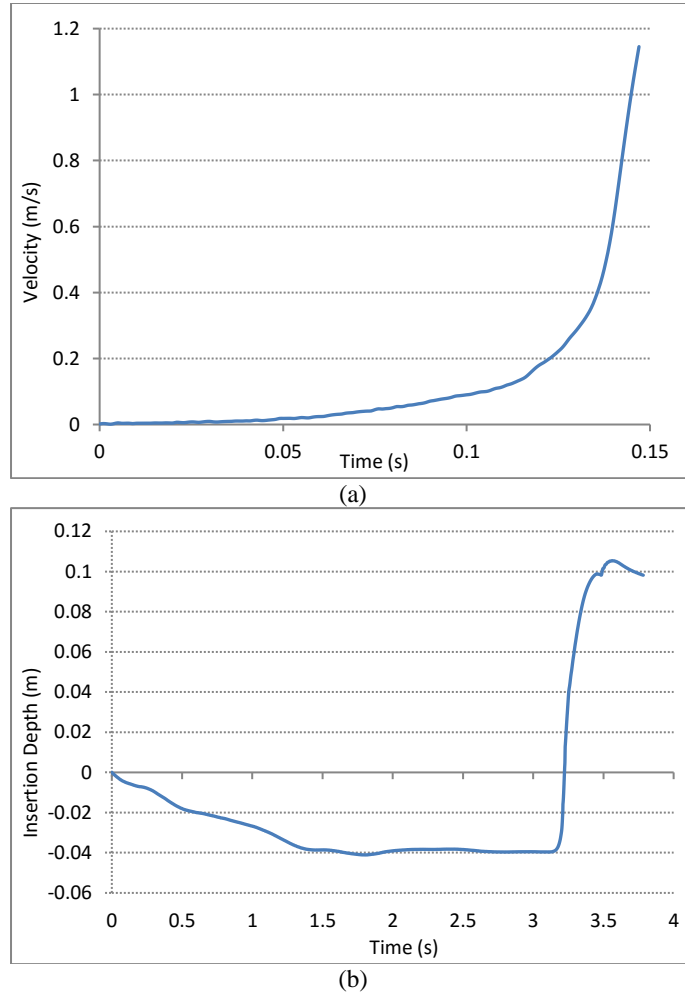


Fig. 4. The ejection experiment. (a) Velocities of haptic stylus increase rapidly from 0.2 m/s to 1.2 m/s within about 0.02 s after it is released suddenly at  $t=0$  s. (b) Changes in insertion depth over time in the virtual wall experiment. The haptic stylus is ejected from  $Z=-0.039$  m to about 0.1 m within 0.25 s after it is released suddenly at  $t=3.15$  s.

#### 4.2 Maximum Ejection Velocity (MEV)

Another experiment is conducted to investigate the relationship between the stiffness of the virtual wall and MEV. The stiffness of the virtual wall is varied from 0.2k to 1k N/m with a step size of 0.1k N/m. Note that the minimum stiffness is subject to the maximum insertion depth, which is in turn limited by the maximum force (around 7.8 N) and workspace size of the haptic device. In the experiment, indentation is made progressively until the maximum force is reached. The haptic stylus is then released to determine the value of MEV during the experiments. The procedure is repeated four times for each stiffness value. It can be seen from Fig. 5(a) that the value of MEV decreases as the stiffness increases, which can be explained by the approximation given below, assuming the potential energy are completely converted

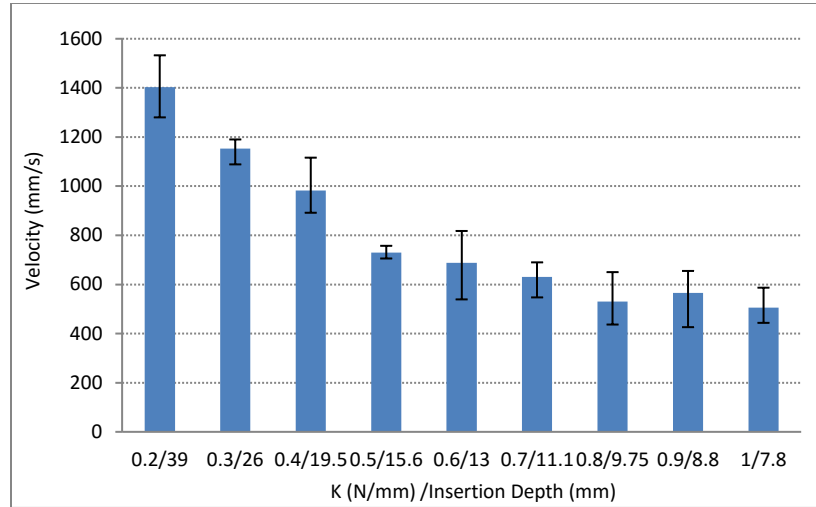
into the kinetic energy,

$$\frac{mV_m^2}{2} \propto \frac{F_m D}{2} = \frac{F_m^2}{2K} \Rightarrow V_m \propto \frac{F_m}{\sqrt{mK}}, \quad (16)$$

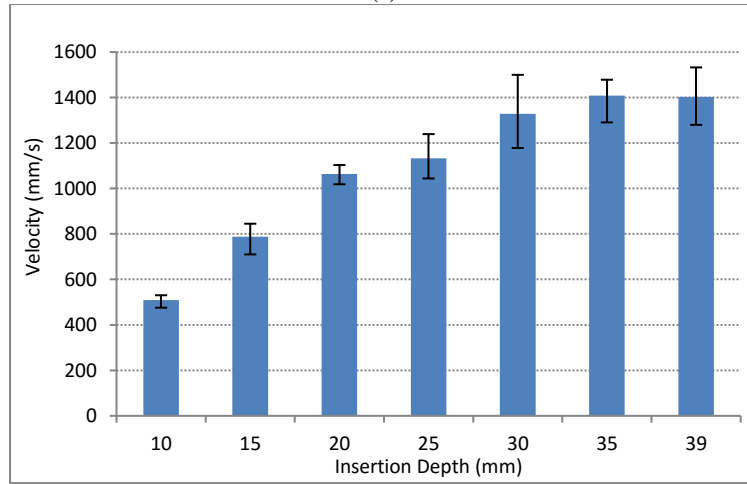
where  $F_m$  is the maximum force exerted on the haptic device,  $m$  is the stylus inertial mass (Eq. (3)),  $K$  is the stiffness, and  $D$  is the penetration depth. It can be seen from Fig. 5(a) that when the stiffness is 0.2k N/m and the insertion depth is 0.039 m, the MEV can reach as high as 1.4 m/s. When the stiffness is increased to 1k N/m, the value of MEV is around 0.5 m/s. This finding indicates that while small stiffness is usually preferred by many stable haptic rendering algorithms, e.g. virtual coupling, it is prone to safety problems. Hence, safety control is indispensable to the scenarios associated with soft objects or small stiffness.

Next, experiments are carried out with the same settings but to study the relationship between MEV and insertion depth. In these experiments, the stiffness is set to 0.2k N/m to enable deepest insertion with the haptic device. The insertion depths range from 0.01 m to 0.039 m. For each insertion depth, the ejection experiment is performed four times. The statistical data are plotted in Fig. 5(b), which shows that the MEV is nearly proportional to the insertion depth  $D$  as it increases from 0.01 m to 0.035 m. This can be explained by the approximation given below,

$$\frac{mV_m^2}{2} \propto \frac{KD^2}{2} \Rightarrow V_m \propto \sqrt{\frac{K}{m}} D. \quad (17)$$



(a)



(b)

Fig. 5. MEV experiments. (a) The relationship between the stylus MEV and stiffness of virtual wall. (b) Variation in MEV with insertion depth ( $K = 200$  N/m).

### 4.3 Safety Observers

Based on the results in the previous experiments, with  $K = 200$  N/m,  $D=0.039$  m, the energy observed by SO, WSO and HGO are calculated and shown in Fig. 6(a) and (b) respectively. It can be seen from Fig. 6(a) that the SO cannot detect the release of haptic stylus even after more than 0.06 s, which is attributed to the large amount of energy accumulated during the insertion procedure. In the figure, the positive energy indicates that the system remains passive even after the hand has released the stylus more than 0.06 s. In contrast to SO, WSO can overcome this issue as evident from Fig. 6(a). It is able to detect the release of hand at  $t=0.036$  s as indicated by the red point, given the energy threshold  $\delta=-0.03$  N-m. For HGO, the graph in Fig. 6(b) shows, with  $\zeta=1.5$  in Eq. (8), that the hand has released the haptic stylus at

$t = 0.048$  s where the value of HGO approaches 1.5, indicating that the hand releases the stylus.

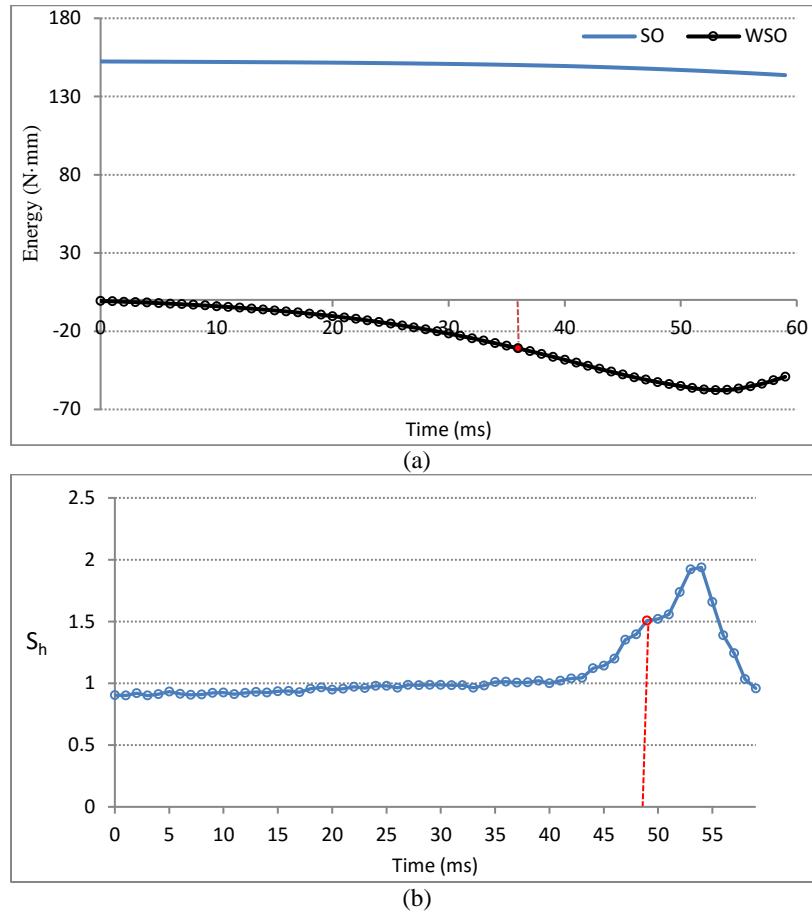


Fig. 6. Safety observers ( $K = 200$  N/m,  $D=0.039$  m). (a) Changes in  $E_{SO}$  after the haptic stylus is released at  $t=0$  s; and trends of  $E_{WSO}$  after the haptic stylus is released at  $t=0$  s ( $w= 100$ ,  $\Delta T=0.001$  s,  $\eta=0.5$ ). (b) Changes in  $S_h$  after the haptic stylus is released at  $t=0$  s ( $\zeta=1.5$ ).

## 4.4 Safety Controllers

### 4.4.1 VFC

The VFC is evaluated by the virtual wall experiments. In the first experiment, a user holds tightly the stylus of the haptic interface to push the wall. This experiment is used to test if the controller will give false alarms during the normal operations. The velocities and forces of a trial are plotted as shown in Fig. 7. The maximum force (about 0.285 m/s) occurs at the pick-up stage. During the push stage, the force increases from 0 N to about 4.5 N within 0.54 s. The threshold of  $V_t$  must be carefully selected when the controller is applied. If the thresholds are too small (e.g.  $V_t = 0.14$  m/s), the controller will be triggered at normal operation as indicated by the circle in Fig. 7. On the other hand, if the thresholds are too large, the controller will not function as ejection occurs. It is found that if the thresholds are set as,  $V_t = 0.6$  m/s and

$F_t = 1$  N, the controller will not be triggered during normal operations.

The proposed controller is then applied to the ejection experiments to evaluate its performance. The variation in velocity of the stylus is plotted in Fig. 8. The stylus are released suddenly after it is pushed into the virtual wall at time  $t=0$  s. Then, the stylus is ejected and the velocity increases from 0 to about 0.6 m/s at time  $t = 0.073$  s. At that time, as indicated by the red circle in the figure, VFC is triggered. After that, the velocity continues to increase and reach the maximum value of 0.75 m/s at  $t=0.075$  s and then reduce rapidly. From this experiment, we can see that since the performance of VFC is directly affected by the suitable selection of threshold, it does not satisfactorily reduce the risk of stylus ejection.

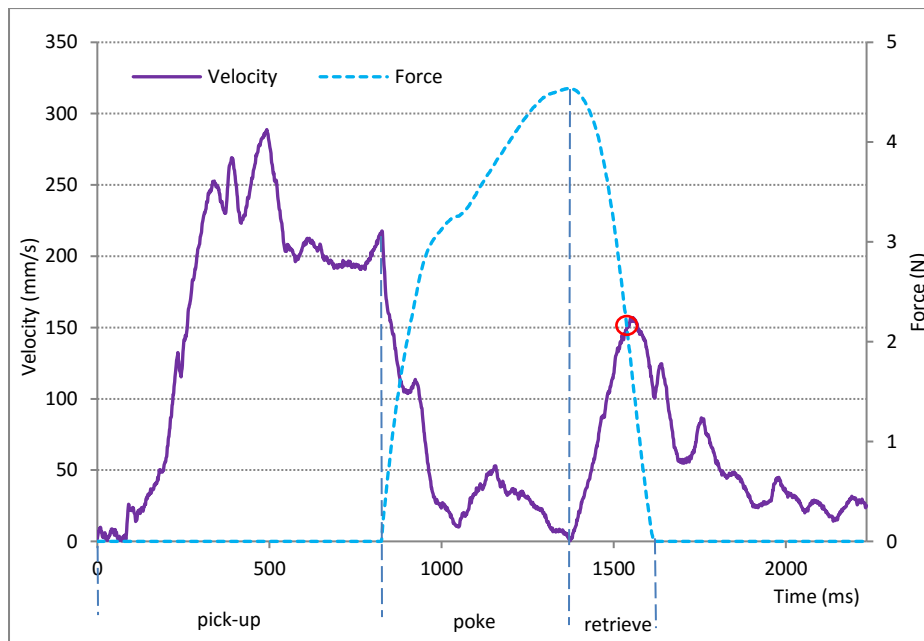


Fig. 7. Velocity and force plots during normal wall-pushing experiments without applying the controller ( $K = 200$  N/m,  $B=0$  N·S/m).

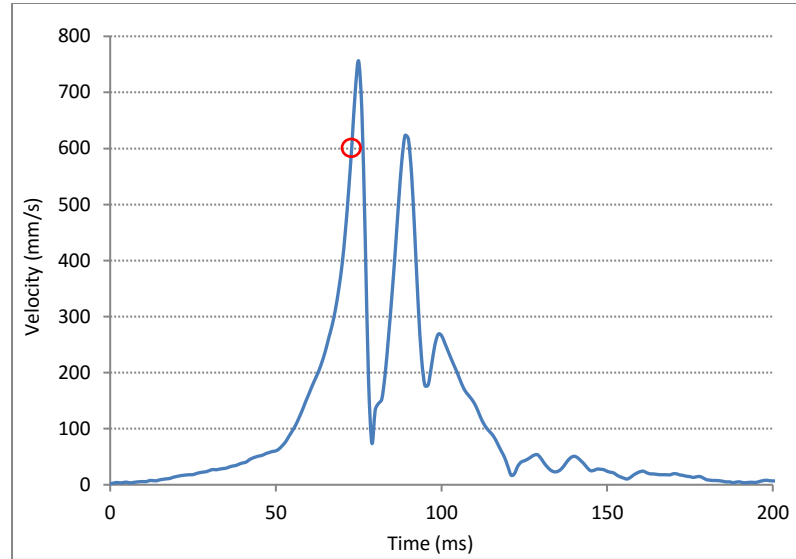
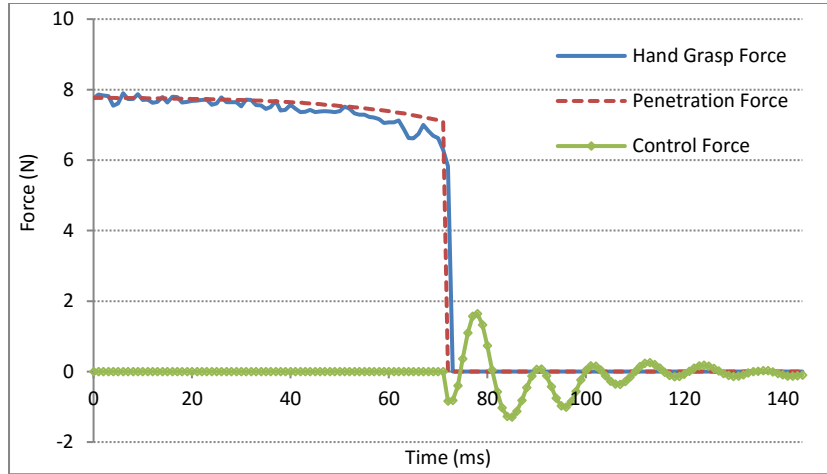


Fig. 8. Velocity plots during the ejection experiment with applying VFC ( $K = 200$  N/m,  $B=0$  N·S/m,  $\mu=5$  N·s/m).

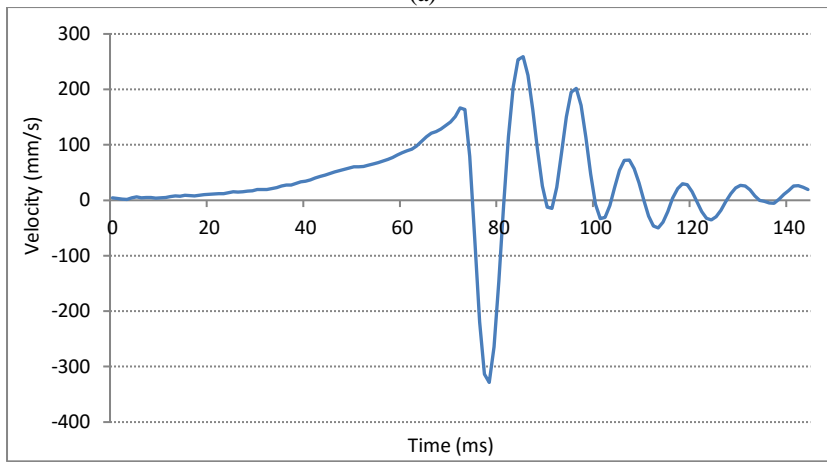
#### 4.4.2 HSC and WSC

The safety controllers proposed based on WSO and HGO are evaluated as well. Fig. 9(a) shows the changes in hand grasp forces, penetration forces and control forces over time based on the HGO method. After the stylus is released at  $t=0$  s, the hand grasp forces follow the penetration forces, and the control force is zero in the initial phase. After HGO detects hand release at  $t=0.072$  s, the penetration force is set to zero and a damping force is introduced to slow down the ejection of haptic stylus. As can be seen from Fig. 9(b), the ejection velocity is decreased from about 1.4 m/s (without safety control as shown in Fig. 5(a)) to about 0.3 m/s.

The safety controller based on WSO is also evaluated. The penetration and control forces are plotted in Fig. 10(a) and (b). The velocity-time plots of the three controllers are presented in Fig. 10(c). From the comparisons of the controlled MEVs as shown in Fig. 11, it can be seen that there is no obvious performance difference between WSC and HSC. Whereas the MEV of VFC is almost two times larger than that of WSC and HSC. Hence, WSC and HSC can perform better with regards to the controlled MEV.



(a)



(b)

Fig. 9. Plots of HSC ( $K = 200 \text{ N/m}$ ,  $D=0.039 \text{ m}$ ,  $\zeta=1.5$ ,  $\mu=5 \text{ N}\cdot\text{s/m}$ ). (a) Variations in hand grasp force, penetration force and control force with time based on the proposed HGO. (b) Velocities of haptic stylus after safety control based on HGO is applied.

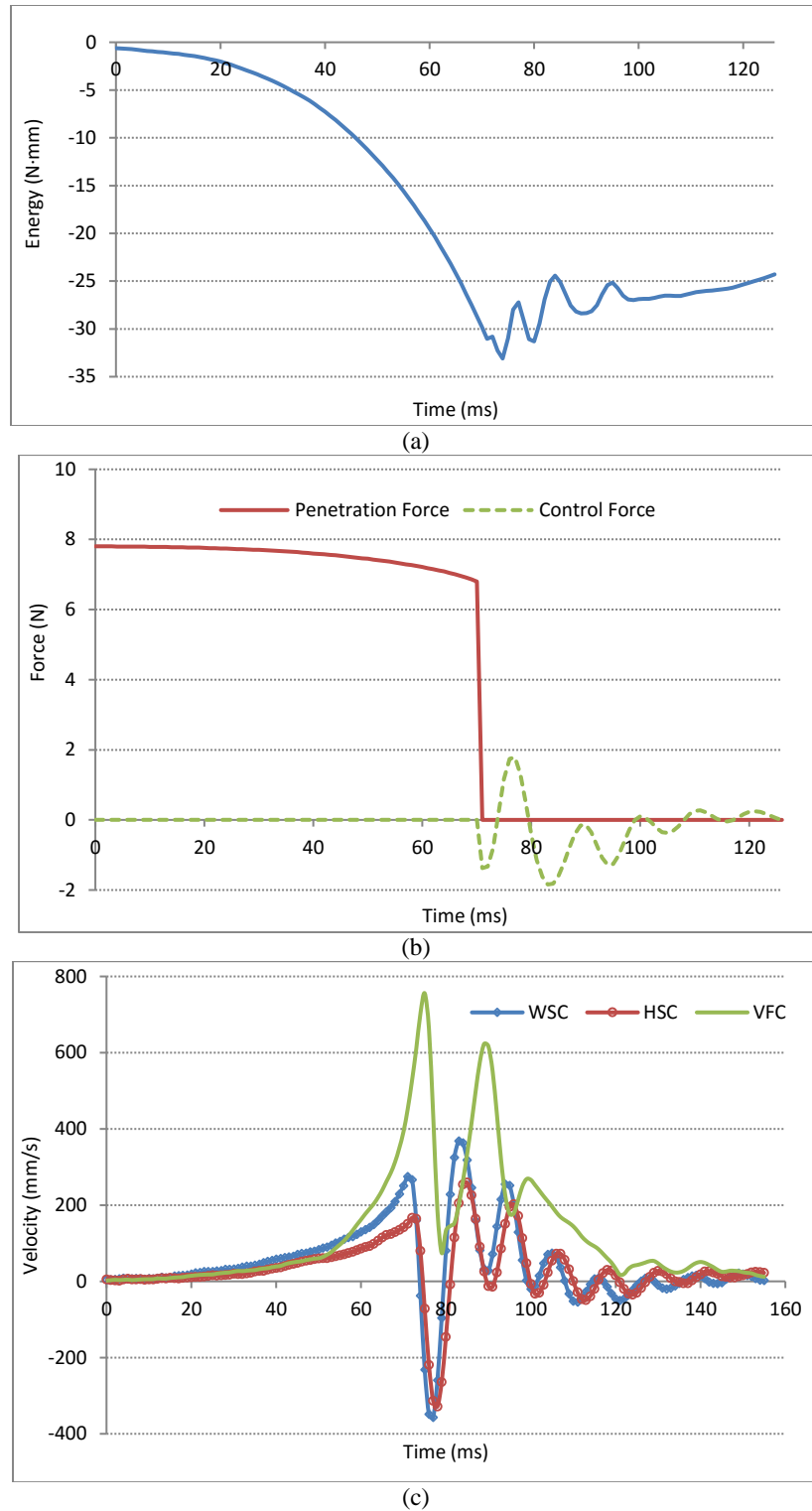


Fig. 10. Plots of WSC ( $w = 100$ ,  $\Delta T=0.001$  s,  $K = 200$  N/m,  $D=0.039$  m,  $\delta=-0.03$  N·m,  $\eta=0.5$ ,  $\mu=5$  N·s/m). (a) Energy observed by WSO with the haptic stylus released at  $t=0$  s. (b) Penetration and control forces measured based on WSC. (c) Velocity changes of haptic stylus after safety controllers are applied.

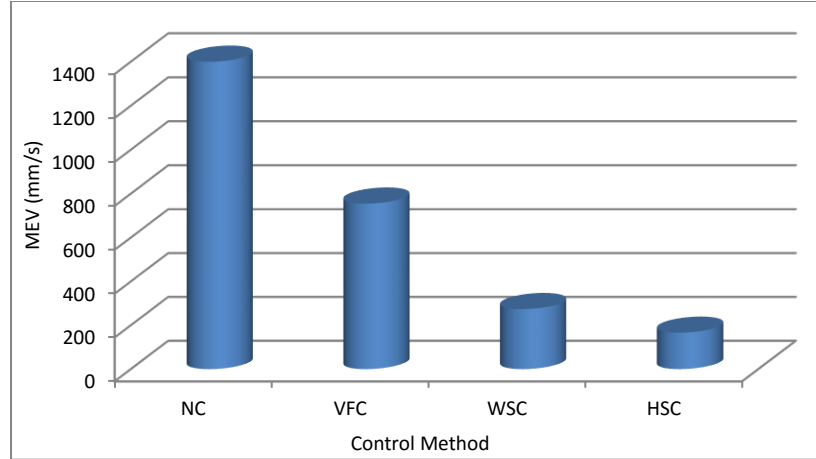


Fig. 11. Comparisons of the controlled MEVs. Note that *NC* means “no controller” is applied in the ejection experiment.

It is interesting to note that the choice of  $w$  does not significantly affect the sensitivity of the safety controller within a certain range as shown in Table 1. In the experiments, the following parameters are used:  $\{K = 200 \text{ N/m}, D=0.039 \text{ m}, \delta=-0.03 \text{ N}\cdot\text{m}, \eta=0.5, \mu=5 \text{ N}\cdot\text{s/m}, \Delta T=0.001 \text{ s}\}$ . As can be seen from the table, when  $w \leq 1000$ , the values of controlled maximum velocity remain relatively low ( $\leq 0.52 \text{ m/s}$ ). As  $w$  increases, the velocities increase as well, meaning the efficiency of the safety controller degrades. Based on the observation,  $w$  is suggested to be set in the range (50, 1000).

Table 1. The relationship between  $w$  and the controlled maximum ejection velocities.

$w$	50	100	200	500	1000	2000	4000	5000	6000	10000
MEV (m/s)	0.438	0.357	0.348	0.35	0.52	0.549	0.739	0.823	1.096	1.094

#### 4.5 Active Force Experiments

The following experiments are designed to investigate the performance of the proposed safety control strategies for the systems with active forces. In the experiments, a sinusoidal force ( $f=\sin(5t)$ ) is applied to the haptic stylus along the Z axis. If the stylus is let go in free space at  $t=0 \text{ s}$ , then, it will move with a high velocity within a short period of time (around  $1.1 \text{ m/s}$  at  $t=0.17 \text{ s}$ ) as shown in Fig. 12. If the user grasps the stylus tightly, with  $\delta=-0.005 \text{ N}\cdot\text{m}$ , the graph depicting the changes in energy observed by WSO with time in Fig. 13 shows that the energy fluctuates around zero and passivity is maintained. If the user suddenly releases the stylus, WSO can detect the change with a negative peak at about  $t=1.35 \text{ s}$  as shown in Fig. 14(a), indicating that the system is very active. By applying the safety control strategy, the effect is suppressed and the MEV is decreased to  $0.18 \text{ m/s}$  (see Fig. 14(b)).

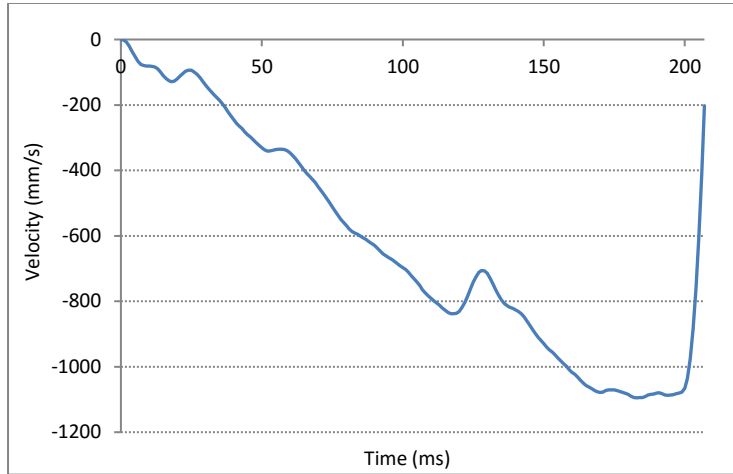


Fig. 12. Velocity of haptic stylus when a sinusoidal force is applied and the stylus is released at  $t=0$  s.

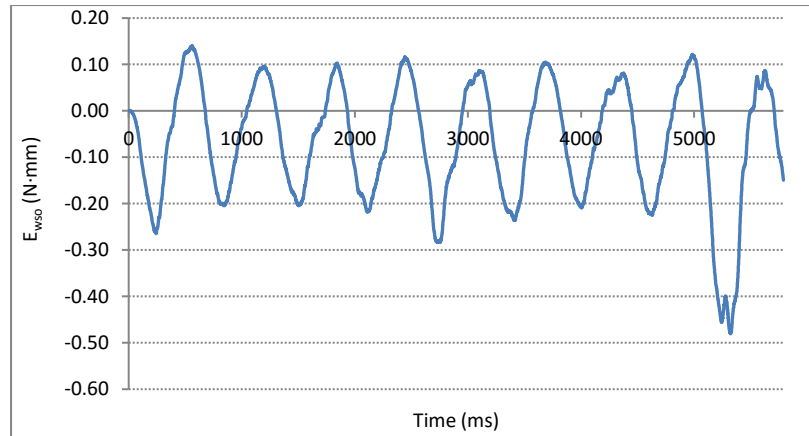


Fig. 13. Energy observed by WSO ( $w=100$ ,  $\Delta T=0.001$  s) when a sinusoidal force is applied and the stylus is gripped tightly.

On the other hand, the effect of active force amplitude on WSO is studied. Fig. 14(c) shows the results of the experiment where active forces with different amplitudes from 1 N to 5 N are applied to the tightly gripped haptic stylus. The magnitude of the observed energy by WSO increases with the active force amplitude. Hence, the energy threshold  $\delta$  (a negative value) in Eq. (10) should be set properly, depending on the maximum active force applied, to reduce the sensitivity of WSO.

Similarly, the safety control strategy based on HGO is also investigated. When the hand grips the stylus tightly, the values of HGO are below 1 as shown in Fig. 15(a). After the stylus is released at  $t=1.35$  s, the values of HGO increase to reach the threshold value  $\zeta=1.5$  and the safety controller is triggered at that moment. As a result, the MEV is controlled to less than 0.3 m/s (see Fig. 15(b) which is far below the

uncontrolled value 1.1 m/s (see Fig. 12).

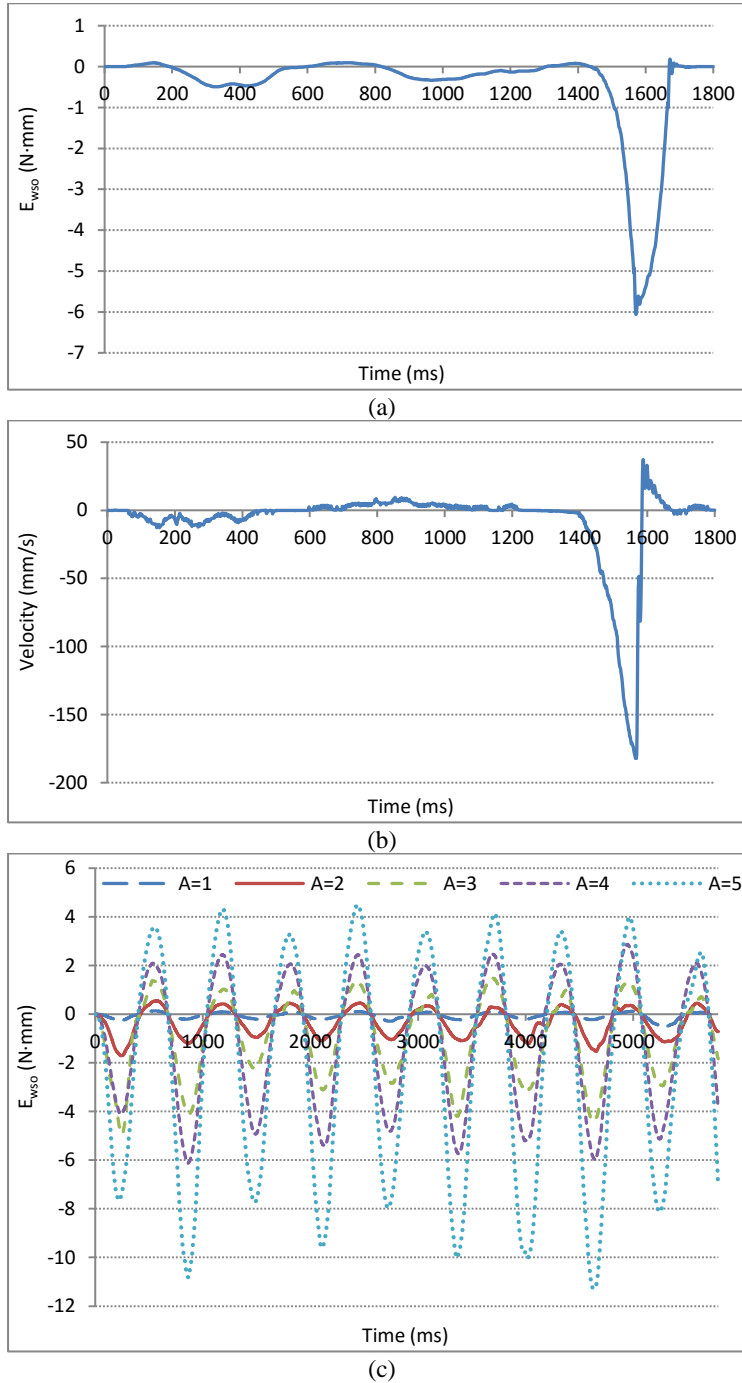


Fig. 14. Plots of WSO ( $w = 100$ ,  $\Delta T = 0.001$  s,  $\delta = -0.005$  N·m,  $\eta = 0.5$ ). (a) Energy observed by WSO when a sinusoidal force is applied and the stylus is grasped until  $t = 1.35$  s. (b) Velocity changes of the haptic stylus being grasped until  $t = 1.35$  s. Safety controller based on WSO is applied. (c) Energy observed by WSO with sinusoidal forces of amplitudes from 1 N to 5 N applied to the tightly grasped stylus.

Finally, the relationship between HGO and the active force amplitude is investigated. The results in Fig. 15 (c) show that the system remains relatively stable ( $S_h \sim 1$ ) when the stylus is grasped tightly. From these experiments, it can be concluded that the safety control strategies based on WSO and HGO can both successfully decrease the risks that may happen in the systems with active forces.

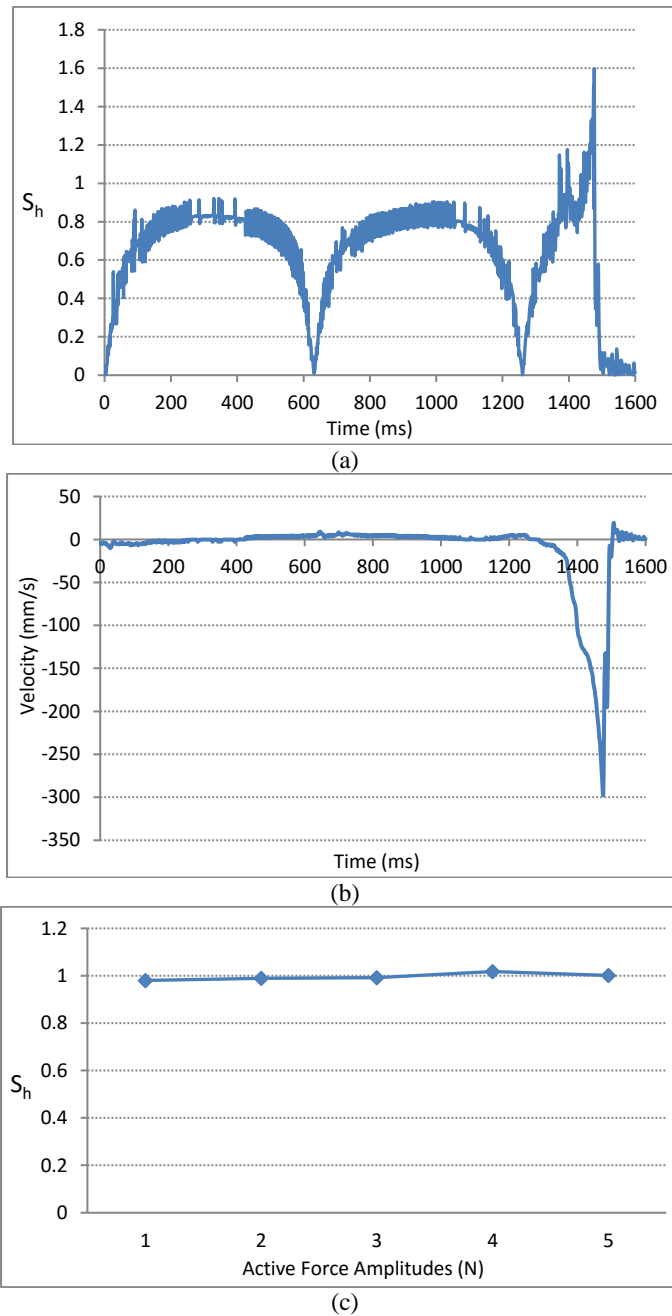


Fig. 15. Plots of HGO ( $\zeta=1.5$ ). (a) The observed HGO with a sinusoidal force applied (the stylus is grasped tightly until  $t=1.35$  s). (b) Velocity changes of haptic stylus being grasped until  $t=1.35$  s. Safety controller based on HGO is applied to the tightly grasped stylus. (c) Variations in  $S_h$  with active force amplitudes: sinusoidal forces of amplitudes from 1 to 5 N are applied to the tightly gripped stylus.

## 5 DISCUSSIONS

In this study, three haptic safety-control models are proposed and evaluated with experiments using a specific impedance haptic device, the PHANTOM<sup>®</sup> Desktop<sup>™</sup>. The methods are also applicable to other kinds of impedance haptic devices. However, the parameters in the proposed hand grasp force model need to be carefully tuned for individual devices to guarantee the accuracy of the safety controller. Notice that the mass  $m$  in the hand grasp force model is not given by the value of inertia (apparent mass of stylus) provided in the specification of PHANTOM<sup>®</sup> Desktop<sup>™</sup>. One possible reason of this discrepancy is that this apparent mass as defined by the specification was measured while the stylus is freely manipulated in a virtual environment [33], which is different from the scenario in our experiment. In contrast, the inertia is approximated based on the relationship between MEV, insertion depth and stiffness obtained from the ejection experiment. The estimated value of  $m$  is 0.157 kg, which is much larger than the inertia value 0.045 kg as stated in the specification. Note that in the calculation, it is assumed that the total potential energy generated by pushing the tip of the stylus into the virtual wall is completely converted to the kinetic energy. Due to energy loss, the real physical inertia shall be less than the calculated one.

Comparing Fig. 8, Fig. 9(b) and Fig. 10(c), we can find that the maximum velocity of the stylus is still relatively large even though VFC is applied. As shown in Eq. (1), the performance of VFC is directly affected by the choice of velocity threshold. The threshold value could not be too small, otherwise the controller will be incorrectly triggered and disturb normal operations of the haptic interface. When there are no rapid operations performed via the stylus, the threshold value of 0.6 m/s used in the paper is considered appropriate. Otherwise, the threshold must be increased to allow VFC to function, e.g. a user pushes the stylus against a wall with a high velocity larger than 0.6 m/s. However, the increase in threshold value also causes VFC to become inefficient to reduce the ejection velocities. In contrast, HSC and WSC are not velocity-sensitive since they also take into account the forces and energy in the protection mechanism. Nevertheless, the performance of HSC and WSC are also dependent on the setting of other thresholds, i.e.  $\zeta$  in Eq. (8) and  $\delta$  in Eq. (13), which shall also be carefully tuned in order to enable the controllers to function properly. As mentioned in the previous section, WSO is sensitive to the amplitude of active forces. As a result, the threshold energy (with a negative value) that determines whether the system is safe or not should be set properly. If the threshold energy is too small, then, the safety controller may not suppress the ejection of haptic stylus effectively and the protection is likely to fail. If the

threshold energy is too large, the safety controller may apply protection force unnecessarily when the user is already interacting with the virtual environment in a safe manner. Although the HGO model is not sensitive to the maximum active force, the parameters used in Eq. (5) and (8) also need to be tuned carefully for different haptic devices. The following guidelines are used to tune the parameters in order to design a sensitive safety controller:

- In normal operations, the controller is not triggered. For example, a user manipulates the stylus of a haptic device in a free space with relatively large velocities, it is considered as a normal operation. When a user slides the tip on a virtual object, the operation should not be disturbed.
- The controller detects abnormal operations timely. If a user grasps the stylus and punches it to a virtual object with a large velocity, or the stylus is released suddenly when a large force is being applied, the controller shall be triggered and the corresponding protection actions should be performed.
- In abnormal cases, the controller greatly decreases the velocity or momentum to minimize the harmful effect.

Based on the above guidelines, the procedure of tuning the thresholds is thus provided:

- Firstly, find the boundary value of safety observer in normal operations. In VFC, for example, it is necessary to find the appropriate threshold  $V_t$ . For a specific task, the maximum velocities  $V_m$  are recorded under normal operations. Since the values may vary with different users, it is recommended to conduct multiple experiments with enough numbers of users.
- After the boundary value is obtained, the threshold is initially set to that value. Then, under abnormal operations, it needs to check if this initial threshold can work properly or not. If the safety controller cannot detect the abnormal cases in time, or the protection is insufficient, then, the threshold needs to be adjusted. For example, in VFC, the threshold  $V_t$  could be decreased by a amount based on statistical values of  $V_m$ . This threshold adjustment procedure minimizes the possibility that the controller give false alarm during normal operations.

In the WSO model, the hand velocity is approximated by the velocity of the stylus as shown in Eq. (A.2) (see Appendix). This approximation is reasonable when the user grips the stylus tightly. When the stylus is released, the grasp force approaches zero very quickly, whereas the velocity of the stylus increases rapidly and can no longer approximate the hand velocity. Nevertheless, the duration for which the stylus

is completely released from the user's hand is very short (e.g. 50 ms); the energy produced after that moment indeed has little contribution to the control strategy since the safety controller has already been triggered.

The damping model in Eq. (13) and (14) is a simple yet effective approach developed for the proposed safety controllers, as evident from the experimental results. More effective control approaches can also be proposed based on the values of HGO or WSO. Further research will be conducted to develop improved versions of safety control methods.

## 6 CONCLUSIONS

In this paper, safety control models based on VFO, HGO and WSO are proposed for haptics-enabled system. The controllers do not require prior knowledge of virtual environments and additional hardware sensors to detect system instability. They can also be applied to the haptics-enabled systems with active forces. VFC is directly derived from traditional safety control algorithms. One evident disadvantage of the controller is that it is directly affected by the setting of the velocity threshold and leads to sub-optimal performance. In contrast, both HGO and WSO are based on the proposed hand grasp force model – the former directly estimates the hand grasp status and the latter makes use of passivity analysis but relaxing the restriction of passivity. WSO features local monitoring of system passivity in the time domain, which makes the safety controller sensitive and robust to the changes of user's inputs and virtual environments. It is also sensitive to the changes of active forces whilst HGO is relative stable and robust to the variations of active force amplitude. The experiments clearly demonstrate that the proposed safety control models can greatly eliminate instability in haptic rendering, even with active forces. With these advantages, it has the potential to be used for a wide range of haptics-enabled applications.

As haptic technology is increasingly adopted in various applications and virtual environments are becoming more complex, safety control is indispensable to protect both haptic systems and users. Based on the proposed safety control models, further research will be conducted for the following three typical haptics-enabled situations. The first is a system containing dynamic objects commonly involved in most physics-based simulations, where the system stability can be easily perturbed by the dynamics. The second concerns haptic playback systems [31] where pre-recorded forces and positional trajectories of different ranges are fed into the haptic devices. Conventional passivity analysis is not applicable to such

active haptic systems. Lastly, haptics-enabled tele-operation systems [4], susceptible to stochastic character and uncertainty of network transmission, will also be studied to investigate the effect of the safety control strategies on the systems. For instance, it is necessary to ensure a forceful push from a remote environment is safely transmitted to the local user.

## ACKNOWLEDGMENTS

This work was supported in part by the Research Grants Council of Hong Kong SAR (Project No. PolyU 5134/12E, 5152/09E) and the Hong Kong Polytechnic University (Project Account Code 87RF).

## REFERENCES

1. Adams, R.J. and B. Hannaford, *Stable haptic interaction with virtual environments*. Robotics and Automation, IEEE Transactions on, 1999. **15**(3): p. 465-474.
2. Adams, R.J., M.R. Moreyra, and B. Hannaford. *Stability and performance of haptic displays: Theory and experiments*. in *Proceedings ASME International Mechanical Engineering Congress and Exhibition*. 1998.
3. Stramigioli, S., et al. *A novel theory for sampled data system passivity*. in *Intelligent Robots and Systems, 2002. IEEE/RSJ International Conference on*. 2002. IEEE.
4. Ware, J., et al. *Experimental studies on improving safety in haptic and teleoperation systems*. in *American Control Conference, 2009. ACC'09*. 2009. IEEE.
5. Lin, M.C. and M. Otaduy, *Haptic rendering: Foundations, algorithms and applications*2008: AK Peters, Ltd.
6. Hannaford, B. and J.H. Ryu, *Time-domain passivity control of haptic interfaces*. Robotics and Automation, IEEE Transactions on, 2002. **18**(1): p. 1-10.
7. Colgate, J.E. and G. Schenkel. *Passivity of a class of sampled-data systems: Application to haptic interfaces*. in *American Control Conference, 1994*. 1994. IEEE.
8. Ryu, J.H., et al., *Time domain passivity control with reference energy following*. Control Systems Technology, IEEE Transactions on, 2005. **13**(5): p. 737-742.
9. Diolaiti, N., et al., *Stability of haptic rendering: Discretization, quantization, time delay, and coulomb effects*. Robotics, IEEE Transactions on, 2006. **22**(2): p. 256-268.
10. Ye, Y., et al., *A power-based time domain passivity control for haptic interfaces*. Control Systems Technology, IEEE Transactions on, 2011. **19**(4): p. 874-883.
11. Gillespie, R.B. and M.R. Cutkosky. *Stable user-specific haptic rendering of the virtual wall*. in *Proceedings of the ASME International Mechanical Engineering Congress and Exhibition*. 1996.
12. Champion, G., *On the synthesis of haptic textures*. The Synthesis of Three Dimensional Haptic Textures: Geometry, Control, and Psychophysics, 2011: p. 73-97.
13. Yokokohji, Y., T. Imaida, and T. Yoshikawa. *Bilateral control with energy balance monitoring under time-varying communication delay*. in *Robotics and Automation, 2000. Proceedings. ICRA'00. IEEE International Conference on*. 2000. IEEE.
14. Colgate, J.E., M.C. Stanley, and J.M. Brown. *Issues in the haptic display of tool use*. in *Intelligent Robots and Systems 95. Human Robot Interaction and Cooperative Robots', Proceedings. 1995 IEEE/RSJ International Conference on*. 1995. IEEE.
15. Colgate, J.E. and J.M. Brown. *Factors affecting the z-width of a haptic display*. in *Robotics and Automation, 1994. Proceedings., 1994 IEEE International Conference on*. 1994. IEEE.
16. Vasic, M. and A. Billard. *Safety issues in human-robot interactions*. in *Robotics and Automation (ICRA), 2013 IEEE International Conference on*. 2013. IEEE.
17. Laffranchi, M., N.G. Tsagarakis, and D.G. Caldwell, *Improving Safety of Human-Robot Interaction*

- Through Energy Regulation Control and Passive Compliant Design*. Human Machine Interaction-Getting Closer, 2011.
18. Norouzzadeh, S., T. Lorenz, and S. Hirche. *Towards safe physical human-robot interaction: An online optimal control scheme*. in *RO-MAN, 2012 IEEE*. 2012. IEEE.
  19. Hogan, N., *Impedance control: An approach to manipulation: Part II—Implementation*. Journal of dynamic systems, measurement, and control, 1985. **107**(1): p. 8-16.
  20. Kulić, D. and E.A. Croft, *Real-time safety for human–robot interaction*. Robotics and Autonomous Systems, 2006. **54**(1): p. 1-12.
  21. Kuhn, S., T. Gecks, and D. Henrich. *Velocity control for safe robot guidance based on fused vision and force/torque data*. in *Multisensor Fusion and Integration for Intelligent Systems, 2006 IEEE International Conference on*. 2006. IEEE.
  22. Gadd, C.W., *Use of a Weighted-Impulse Criterion for EstimatiéInjury Hazard*. 1966.
  23. Versace, J., *A review of the severity index*. Proceedings of the 15, 1971.
  24. Haddadin, S., A. Albu-Schäffer, and G. Hirzinger. *Safety Evaluation of Physical Human-Robot Interaction via Crash-Testing*. in *Robotics: Science and Systems*. 2007.
  25. Alami, R., et al. *Safe and dependable physical human-robot interaction in anthropic domains: State of the art and challenges*. in *Proc. IROS*. 2006. Citeseer.
  26. ISO, *Robots and robotic devices -- Safety requirements for industrial robots -- Part 1: Robots*. ISO 10218-1:2011 2011.
  27. ISO, *Robots and robotic devices -- Safety requirements for industrial robots -- Part 2: Robot systems and integration*. ISO 10218-2:2011 2011.
  28. Hogan, N. *Multivariable mechanics of the neuromuscular system*. in *IEEE Annual Conference of the Engineering in Medicine and Biology Society*. 1986.
  29. Mahapatra, S. and M. Zefran. *Stable haptic interaction with switched virtual environments*. in *Robotics and Automation, 2003. Proceedings. ICRA'03. IEEE International Conference on*. 2003. IEEE.
  30. Llewellyn, F., *Some fundamental properties of transmission systems*. Proceedings of the IRE, 1952. **40**(3): p. 271-283.
  31. Corno, M., *Haptic playback: Modeling, controller design, and stability analysis*. 2006.
  32. Fu, M.J. and M. Çavuşoğlu, *Human-Arm-and-Hand-Dynamic Model With Variability Analyses for a Stylus-Based Haptic Interface*. 2012.
  33. Massie, T.H. and J.K. Salisbury. *The phantom haptic interface: A device for probing virtual objects*. in *Proceedings of the ASME winter annual meeting, symposium on haptic interfaces for virtual environment and teleoperator systems*. 1994. Chicago, IL.

## Appendix

Fig.A.1 depicts a two-port network-based passivity analysis, where the sign convention for all forces and velocities is defined when power enters the system ports. The system energy exchange is governed by the following equation [9],

$$\int_0^t F_{hap}(\tau)V_h(\tau)dt = E_p + E_d - E_g, \quad (A.1)$$

where  $F_{hap}$  is the force generated by the haptic interface,  $V_h$  is the hand velocity,  $E_p$  is the energy that is stored in the haptic device,  $E_g$  is the energy generated by the “non-idealities” in the control loop, e.g. discretization, quantization, etc., and  $E_d$  is the energy dissipated by frictions. The excessive energy  $\Delta E$  at time step  $n$  with a sampling time step  $\Delta T$  in a discrete-time form is derived as,

$$\Delta E(n) = E_d(n) - E_g(n) \approx \Delta T \sum_{i=1}^n F_h(i)V(i) - E_p(n). \quad (\text{A.2})$$

Note that in above equation, assuming the stylus of the haptic interface is grasped by the user, the hand velocity  $V_h$  is approximated by the velocity of the haptic stylus  $V$  and the force produced by the haptic interface is replaced by the force  $F_h$  as defined by Eq. (4). When the user interacts with the virtual environment in the active regions, the amount of potential energy  $E_p$  that is converted to kinetic energy ( $E_k$ ) is  $\eta = E_k/E_p$ . The  $E_p$  is approximated by the kinetic energy as  $E_p = E_k/\eta = mV^2/2\eta$ , where  $m$  is the physical inertia of the stylus. From Eq. (A.2), the Safety Observer (SO)  $E_{so}$  is defined by,

$$E_{so}(n) = \Delta E(n) \approx \Delta T \sum_{i=1}^n F_h(i)V(i) - mV(n)^2/2\eta. \quad (\text{A.3})$$

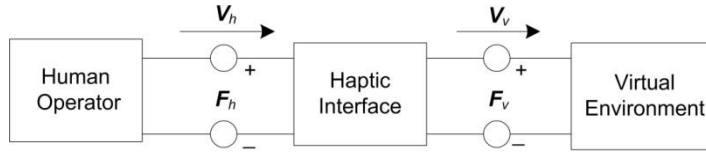


Fig. A.1. Network representation of a haptics-enabled system for passivity analysis.